BILINGUAL PUBLISHING GROUP

Journal of Environmental & Earth Sciences

https://journals.bilpubgroup.com/index.php/jees

ARTICLE

Assessment and Driving Factors of Desertification Vulnerability in the Mu Us Sandy Land, China: A MEDALUS-Based Approach

Yu Ren [1,2], ***Xidong Chen*** [3*]

[1] *Key Laboratory of Ecological Safety and Sustainable Development in Arid Lands, Northwest Institute of Eco-Environment and Resources, Chinese Academy of Sciences, Lanzhou 730000, China*

[2] *University of Chinese Academy of Sciences, Beijing 100049, China*

[3] *Henan Provincial Key Laboratory of Hydrosphere and Watershed Water Security, North China University of Water Resources and Electric Power, Zhengzhou 450011, China*

ABSTRACT

As a major worldwide issue, desertification poses significant threats to ecosystem stability and long-term socio-economic growth. Within China, the Mu Us Sandy land represents a crucial region for studying desertification phenomena. Comprehending how desertification risks are distributed spatially and what mechanisms drive them remains fundamental for implementing effective strategies in land management and risk mitigation. Our research evaluated desertification vulnerability across the Mu Us Sandy land by applying the MEDALUS model, while investigating causal factors via geographical detector methodology. Findings indicated that territories with high desertification vulnerability extend across 71,401.7 km², constituting 76.87% of the entire region, while zones facing extreme desertification hazard cover 20,578.9 km² (22.16%), primarily concentrated in a band-like pattern along the western boundary of the Mu Us Sandy land. Among the four primary indicators, management quality emerged as the most significant driver of desertification susceptibility, followed by vegetation quality and soil quality. Additionally, drought resistance, land use intensity, and erosion protection were identified as the key factors driving desertification sensitivity. The investigation offers significant theoretical perspectives that can guide the formulation of enhanced strategies for controlling desertification and promoting sustainable land resource utilization within the Mu Us Sandy land region.

Keywords: Desertification Risk; MEDALUS; Geographical Detector Method; Driving Factors

*CORRESPONDING AUTHOR:

Xidong Chen, Henan Provincial Key Laboratory of Hydrosphere and Watershed Water Security, North China University of Water Resources and Electric Power, Zhengzhou 450011, China; Email: chenxd@radi.ac.cn

ARTICLE INFO

Received: 5 March 2025 | Revised: 15 April 2025 | Accepted: 22 April 2025 | Published Online: 9 June 2025

DOI: https://doi.org/10.30564/jees.v7i6.8974

CITATION

Ren, Y., Chen, X., 2025. Assessment and Driving Factors of Desertification Vulnerability in the Mu Us Sandy Land, China: A MEDALUS-Based Approach. Journal of Environmental & Earth Sciences. 7(6): 213–226. DOI: https://doi.org/10.30564/jees.v7i6.8974

COPYRIGHT

Copyright © 2025 by the author(s). Published by Bilingual Publishing Group. This is an open access article under the Creative Commons Attribution-NonCommercial 4.0 International (CC BY-NC 4.0) License (https://creativecommons.org/licenses/by-nc/4.0/).

1. Introduction

Land degradation manifested as desertification predominantly occurs in arid, semi-arid, and dry sub-humid territories emerging as a worldwide concern that endangers ecosystem integrity and sustainable socio-economic development [1,2]. Studies suggest that exceeding one-quarter of global terrestrial surfaces face desertification threats, propelled by climatic shifts and anthropogenic actions, simultaneously imperiling the subsistence of roughly 25% of humanity worldwide [3,4]. Through multinational cooperation, the UNCCD and 2030 SDGs strive to halt and reverse desertification processes, ensure sustainable management of land resources, and promote worldwide socio-economic advancement [5,6]. Therefore, addressing desertification requires coordinated action from countries worldwide.

Among nations experiencing profound desertification impacts, China ranks prominently, confronting a multifaceted problem influenced by interacting environmental factors, economic developments, and human-induced modifications [7,8]. Data from 2019 reveals that China's desertified territories encompass around 2.57 million km2, representing 26.81% of its total land surface, with major effects particularly evident throughout the arid and semi-arid zones across northwestern, northern, and southwestern regions [9]. Desertification has resulted in substantial economic losses, estimated at around US$6.8 billion annually, and has directly or indirectly affected nearly 400 million people [10]. Despite ongoing efforts, desertification continues to expand in certain areas. To address this challenge, governmental authorities in China have deployed diverse comprehensive approaches against desertification, incorporating policy measures, engineering interventions, technological innovations, legislative systems, and global partnerships. Prominent programs comprise the policy of "converting cultivated land back to forests and grasslands" [11], the extensive three-north protective forest belt initiative [12], and efforts to control sand sources in the Beijing-Tianjin-Hebei region [13]. While these efforts have yielded some progress, desertification remains a pressing challenge, underscoring the need for enhanced management and intervention.

As a focal point for Chinese desertification studies, the Mu Us Sandy Land has garnered considerable scholarly interest over an extended period [14–16]. Characterized by its fragile natural, economic, and social ecosystems [17], the Mu Us Sandy region has been the subject of extensive scientific investigation since the early 20th century. Initial scientific exploration of this territory was performed by Obrucher, a Russian researcher, followed by comprehensive investigations launched by CAS during the late 1950s that examined regional environmental characteristics, aeolian processes, agricultural and pasture stabilization methods, and approaches for sustainable water resource management [18]. The Chinese government initiated the "Three-North" integrated management program in 1981, encompassing agricultural district planning and methodical assessment of farming, animal husbandry, and prairie resources throughout the Mu Us Sandy region. Recent studies have increasingly employed remote sensing technologies to monitor desertification dynamics and landscape transformations in the Mu Us Sandy Land [16,19]. Satellite-derived data have been widely used to analyze temporal variations in desertified areas [16], assess the impact of vegetation changes [20], and classify land cover types [21], providing essential information for ongoing research. A variety of methods have been applied to assess desertification risk in this region. For instance, Wang et al. (2022) evaluated desertification trends from 2000 to 2020 using the Desertification Index (DI); Han et al. (2020) analyzed three decades of desertification dynamics based on the wind-sanding index [15]; and Ji et al. (2023) developed the Desertification Difference Index (DDI), derived from the MSAVI-Albedo model, to assess desertification trends between 1991 and 2021 [16]. However, the diversity of research methodologies has led to considerable variability in findings. Most studies rely solely on single-source remote sensing data, which hampers the integration of natural and anthropogenic factors in desertification assessments. Moreover, comprehensive investigations into the underlying causal mechanisms of desertification remain limited in the existing literature.

To date, the flexible MEDALUS model has regained attention [22]. This model evaluates desertification risk using four key quality indices: soil conditions, vegetation characteristics, climatic factors, and land management practices. Additionally, each quality index is composed of various remote sensing observation variables [22]. The MEDALUS model is recognized for its flexibility, robust-

ness, and integrative capacity. It allows for the selection of context-specific variables and the construction of analytical frameworks that accommodate diverse spatial scales and data sources [23], thereby addressing the issue of singularity in existing desertification evaluation indicators. Additionally, its structure allows for the adaptation of evaluation criteria to region-specific environmental contexts. Nowadays, MEDALUS has been successfully applied to desertification sensitivity assessments in various other regions [3,24]. Hence, our investigation seeks to evaluate desertification vulnerability within the Mu Us Sandy Land by applying the MEDALUS framework, which combines environmental and human-induced elements, while also examining regional causative factors. Our research particularly focuses on: (1) mapping spatial patterns of desertification vulnerability, and (2) quantifying principal contributing factors to desertification processes across the Mu Us Sandy terrain. Results from this analysis will contribute essential theoretical foundations for establishing improved desertification mitigation approaches and advancing sustainable land resource utilization throughout the Mu Us Sandy region.

2. Materials and Methods

2.1. Study Area

The Mu Us Sandy Land, located in northwestern China, spans the provinces of Shaanxi, Ningxia, and Inner Mongolia, lying at the junction of the Loess Plateau and the northwest Desert. The Yellow River defines its eastern boundary while Inner Mongolian grasslands mark its western limits, exemplifying characteristic arid and semi-arid conditions found throughout northern China [14]. The region experiences an arid climate, with annual precipitation ranging from 250 mm in the northwest to 440 mm in the southeast, of which approximately 70% occurs during the summer months. Water resources are scarce, and precipitation is unevenly distributed throughout the year [14,25]. The soils in the Mu Us Sandy Land are diverse, primarily consisting of sandy, grassland, and saline types, all of which are highly susceptible to wind and sand erosion [26]. Such pedological properties, combined with ecosystem fragility throughout the region, establish the Mu Us Sandy Land as a critical zone for desertification investigations and formulation of remediation approaches. The research domain comprises twelve administrative units (counties, cities, and banners) that collectively encompass the Mu Us Sandy Land territory (**Figure 1**).

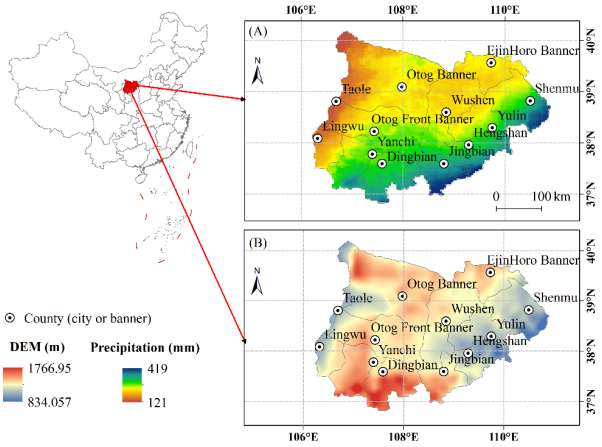

Figure 1. Study Area Overview.

2.2. Data and Pre-Processing

This investigation utilized diverse data repositories addressing four fundamental components: soil characteristics, vegetation parameters, climatic variables, and management factors. Soil data, including information on soil texture (ST), bulk density (SBD), organic carbon content (SOC), rock fragments (RF), and effective soil water content (SWC), were sourced from the Harmonized World Soil Database (version 2.0) (https://gaez.fao.org/pages/hwsd) (spatial resolution: 1km; time resolution: 2020). Surface classification data were obtained from the European Space Agency (ESA) (https://data.ceda.ac.uk/neodc/esacci/land_cover/data) (spatial resolution: 300 m; time resolution: 2020). Normalized Difference Vegetation Index (NDVI) data were derived from the MOD13A1 product (https://search.earthdata.nasa.gov/search) (spatial resolution: 500 m; time resolution: 2020). Precipitation and potential evapotranspiration data were accessed from TerraClimate (https://www.climatologylab.org/terraclimate.html) (spatial resolution: 4 km; time resolution: 2020), while aridity indices were computed as ratios between annual rainfall and evapotranspiration potential according to Equation (1) [27]. Global population density data were sourced from LandScan (https://landscan.ornl.gov/) (spatial resolution: 1 km; time resolution: 2020). To ensure consistency with the study area, these datasets were merged, masked, resampled

at varying resolutions, and finally harmonized to a 1 km resolution.

$$\mathrm{AI} = \frac{E_p}{P} \quad (1)$$

where *AI* is the aridity index, E_P is potential evapotranspiration, and *P* is precipitation.

2.3. Methods

Desertification sensitivity refers to the susceptibility of land to desertification and is typically represented by a Desertification Sensitivity Index (DSI), where higher values indicate greater vulnerability [22,23,28]. In this study, we assessed desertification sensitivity in the Mu Us Sandy Land using the MEDALUS model [23,28], which integrates four key indicators: soil characteristics, vegetation attributes, climatic conditions, and land management practices. The resulting vulnerability indices were categorized into distinct risk levels, with classification reliability subsequently verified through PCA methodologies [29]. To further investigate the drivers of desertification sensitivity, the K-means clustering method combined with geographical detector method to quantify comparative influences among the four major indicators [30,31].

2.3.1. MEDALUS Model

Mu Us Sandy Land is a region subject to pronounced ecological stressors—including arid climate, unconsolidated soil structure, sparse vegetation cover, and intensive anthropogenic disturbance [32,33]. Therefore, we selected soil bulk density (SBD), texture characteristics (ST), rock fragment content (RF), effective soil moisture capacity (SWC), and organic carbon concentration (SOC) to comprise the soil quality index. The above variables can effectively reflect the conditions of the unconsolidated soils [28]. As for vegetation quality index, drought resistance capabilities (DR), erosion prevention potential (EP), fire susceptibility (FR), and NDVI were incorporated following the work of Ferrara et al. (2020) [23]. Then, considering the arid climate characteristics of the Mu Us Sandy region, the climate quality metric was established using precipitation patterns (PRE) and aridity indices (AI), which can reflect the arid climate characteristics [23]. For management quality evaluation index, the land utilization intensity measurement (LUI) and human population distribution density (PD) were used, similar to the previous studies [23,28]. Specifically, the MEDALUS model is calculated as follows: (1) the selected observation variables are segmented into different layers, and appropriate weights are assigned to each variable layer according to the methods outlined in the methodologies by Ferrara et al. (2020) and Ren et al. (2023) [23,34]. Detailed classification criteria and assigned weights for each sub-indicator are provided in **Tables A1**–**A4** of **Appendix A**; (2) then, each quality index (soil, vegetation, climate, and management) is calculated separately according to Equation (2); (3) next, the desertification vulnerability indicator is determined through geometric mean calculation of all four quality parameters (Equation (3)); (4) finally, the desertification risk level is obtained based on the four derived quality indices (Equation (4)).

$$Quality\_x_{ij} = (variable\_1_{ij} \bullet variable\_2_{ij}, \bullet variable\_3_{ij} \ldots . variable\_n_{ij})^{1/n_{ij}} \quad (2)$$

where *i* and *j* indicate the row and column positions of specific pixels for every parameter; *n* refers to the parameter quantity; and *x* corresponds to the four quality indicators: soil, climate, vegetation, and management.

$$DSI_{ij} = (SQI_{ij} \bullet VQI_{ij} \bullet CQI_{ij} \bullet MQI_{ij})^{1/4} \quad (3)$$

where *DSI* is the desertification vulnerability index, and *SQI*, *VQI*, *CQI*, and *MQI* represent the soil, vegetation, climate, and management quality indices, respectively.

2.3.2. Principal Component Analysis

PCA represents a commonly employed statistical technique for dimensionality reduction and extraction of essential features from complex multivariate datasets [29]. This approach converts initial variables into orthogonally independent components while maximizing information preservation from the original dataset [29,35]. These derived components are arranged hierarchically according to explained variance, with successive components capturing decreasing proportions of data variability. In this study, the PCA is used to reveal the relationship between each principal component and the original variables, thereby assessing the model's stability [29]. The main steps include: data standardization (Equation (4)), determination of covari-

ance structures (Equation (5)), computation of eigenvalues and associated eigenvectors (Equation (6)), and principal component score calculation (Equation (7)) [29].

$$z_{ij} = \frac{x_{ij} - \bar{x}_j}{s_j} \tag{4}$$

where Z_{ij} is the standardized value of the i-th sample for the j-th variable, x_{ij} is the original value, $\bar{x}_i$ is the mean of the j-th variable, and S_i is its standard deviation.

$$C = \frac{1}{n-1}\sum_{i=1}^{n}(z_i - \bar{z})(z_i - \bar{z})^T \tag{5}$$

where C corresponds to the covariance matrix, n reflects total sample quantity, z_i is the standardized value of the i-th sample, and $\bar{z}$ constitutes the vector containing mean values across all variables.

$$CV = V\Lambda \tag{6}$$

where C symbolizes the covariance matrix, V denotes the matrix of eigenvectors, and Λ represents the diagonal arrangement of eigenvalues.

$$Y = ZV \tag{7}$$

where Y signifies the matrix of scores, Z identifies the matrix containing normalized data, and V characterizes the matrix composed of eigenvectors.

2.3.3. Desertification Drivers Analysis

Spatial and temporal variations in land degradation vulnerability arise from the interplay of multiple environmental and anthropogenic factors, resulting in distinct spatial distribution patterns. Identifying and understanding these patterns is essential for the effective management and mitigation of desertification processes [36,37]. To statistically examine spatial heterogeneity and quantify the influence of potential driving factors, this study adopts the geographic detector method—an analytical framework widely applied in environmental, ecological, and socio-geographical research domains [38,39]. Prior to conducting factor detection, we employed the K-means clustering algorithm to discretize all continuous indicators into four categorical levels [28], as required by the geographic detector's input format. K-means is a widely used unsupervised machine learning technique that partitions data into K mutually exclusive clusters by minimizing intra-cluster variance and maximizing inter-cluster distinction through iterative optimization (Equation (8)) [40]. This preprocessing step ensures that the spatial variance in land degradation vulnerability can be accurately attributed to the underlying drivers captured by the selected indicators. Following the completion of indicator classification, factor probing is conducted to assess the driving influence of each selected parameter on desertification sensitivity, with the strength of this influence quantified by the q-value metric (Equations (9)–(11)) [31].

$$J = \sum_{i=1}^{K}\sum_{x_j \in C_i} ||x_j - \mu_i||^2 \tag{8}$$

where J is the objective function, representing the sum of squared distances between all points in the cluster and its center of mass. The goal of the K-means algorithm is to minimize J through iterative optimization, adjusting the center of mass to bring data points closer to it. C_i is the i-th cluster, containing all data points x_i, and μ_i is the center of mass of cluster i, the mean of all points in C_i, $||x_j - \mu_i||^2$ is the squared Euclidean distance between data point x_i and center μ_i.

$$q = 1 - \frac{\sum_{i=1}^{L} N_i \sigma_i^2}{N\sigma^2} = 1 - \frac{SSW}{SST} \tag{9}$$

$$SSW = \sum_{i=1}^{L} N_i \sigma_i^2 \tag{10}$$

$$SST = N\sigma^2 \tag{11}$$

where i represents the classification layer of response or predictor variables; N_i and N refers to variance of the dependent variable in stratum, and indicates this variance across the entire studied area; σ_i^2 and σ^2 respectively represent the response variable's variance in classification layer i and across the entire study territory. SSW and SST denote the within-stratum variance and total variance of the region, respectively. Values of q fall between [0, 1], whereby greater values suggest enhanced explanatory capability of independent variables regarding the dependent variable.

3. Results

3.1. Soil, Vegetation, Climate, and Management Quality Indexes

Utilizing the MEDALUS framework, our study generated quality index maps for soil (**Figure 2(A)**), vegetation quality index map (**Figure 2(B)**), climate quality index map (**Figure 2(C)**), and management quality index map (**Figure 2(D)**). Our analysis indicates that the Mu Us Sandy Land regions exhibiting degraded soil quality mainly occur in central areas, encompassing Wushen County, western Yulin County, and eastern portions of Otog Front Banner. Vegetation degradation primarily appears in northwestern Otog Banner and south-central sections of Otog Front Banner. The western portion of the Mu Us Sandy Land, comprising Taole County, Lingwu County, and western Otog Banner, exhibits concentrated areas of suboptimal climate conditions. Inadequate management practices appear more scattered throughout the region, with particular prominence in western Lingwu County and northern Jingbian County (**Figure 2**).

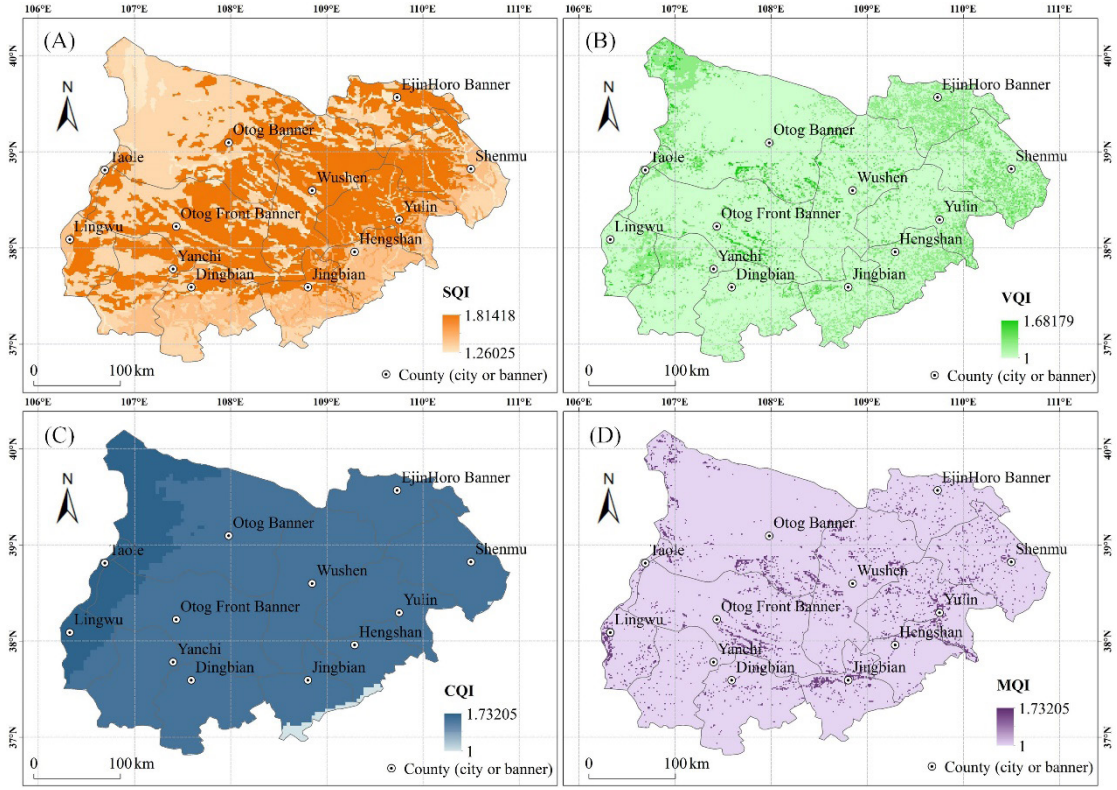

Figure 2. Quality Index Distributions Across the Mu Us Sandy Land: (**A**) Soil Quality Assessment, (**B**) Vegetation Quality Evaluation, (**C**) Climate Quality Measurement, (**D**) Management Quality Appraisal.

3.2. Spatial Patterns of Desertification Risk across The Mu Us Sandy Land

Figure 3 presents geographic patterns of desertification vulnerability across the Mu Us Sandy Land. The desertification sensitivity index was computed from soil, vegetation, climate, and management quality indicators (**Figure 3(A)**) then categorized into vulnerability levels according to standards established by Ferrara et al. (2020) and Ren et al. (2024) (**Figure 3(B)**) [23,28]. A total of 4,000 sample points were randomly generated with a minimum distance of 1 km, and principal component analysis (**Figure 4**) was performed. The principal component analysis score plot (**Figure 4(A)**) shows that the three principal components (PC1: 25.6%; PC2: 19.4%; PC3: 15.2%) explained 60.2% of the total variance, indicating a credible result [23]. The 95% confidence interval analysis showed a significant clustering effect, with most categories well within the interval, confirming the reliability of the classification. The loading plot of principal component analysis (**Figure 4(B)**)

shows that the dominant variables accounting for PC1 are DSI (0.41), LUI (0.40), EP (0.38), DR (0.36), MQI (0.33), and VQI (0.31); the dominant variables for PC2 are SBD (0.48), ST (0.42), and SQI (0.42); and those for PC3 are AI (0.43), PRE (0.43), and CQI (0.34).

Additionally, we computed the area and percentage of each risk class (**Table 1**). Our findings show that moderate-risk desertification zones comprise 904.80 km² (0.97%) of the Mu Us Sandy Land, predominantly appearing along southern boundaries of Jingbian and Hengshan counties. The high-risk area spanned 71,401.70 km² (76.87%), representing the largest proportion and widespread distribution. The extreme-risk area totaled 20,578.88 km² (22.16%), primarily located along the western edge of the Mu Us Sandy Land, including the northwest of Lingwu County, Taole County, and the western part of Otog Front Banner, with some sporadic occurrences in the central region.

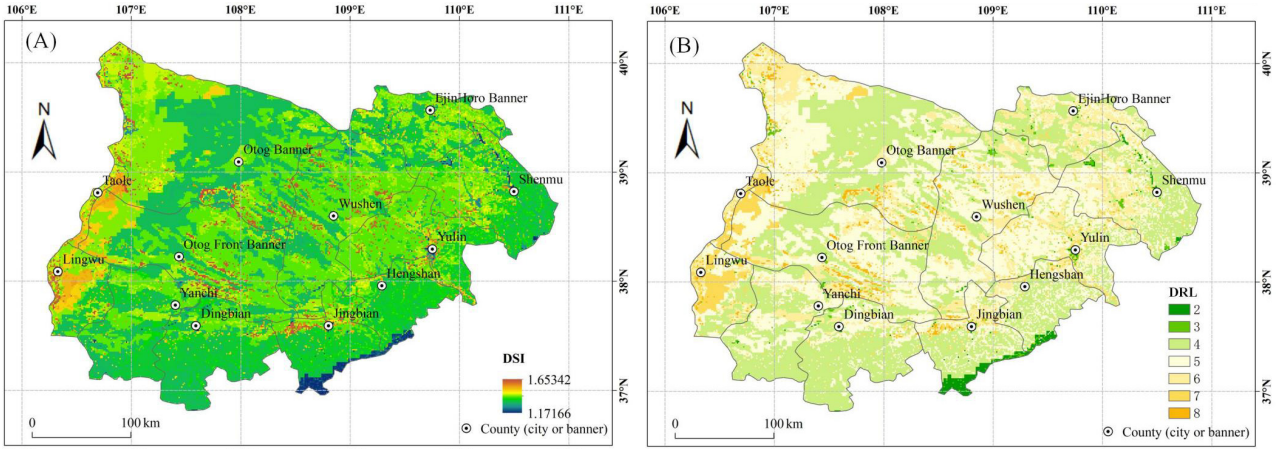

Figure 3. Geographic Patterns of Desertification Vulnerability Across the Mu Us Sandy Land. (**A**) Mapping of Desertification Sensitivity Index (DSI). (**B**) Spatial Distribution of Desertification Risk, DRL Represents the Desertification Risk Level, with Higher Level Indicating Greater Desertification Risk.

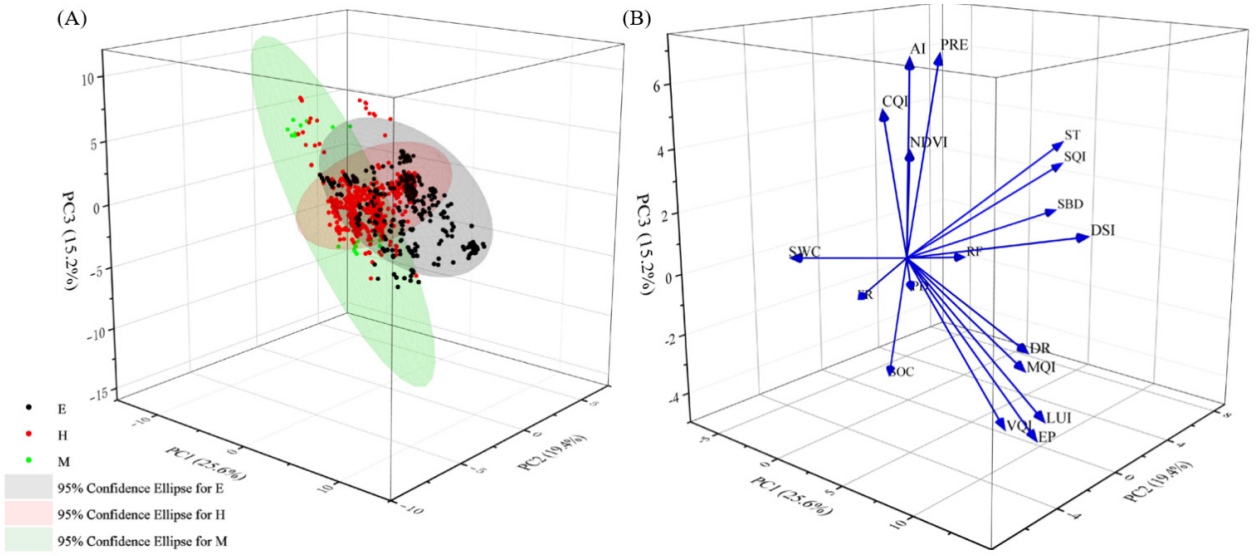

Figure 4. Results of Principal Component Analysis. (**A**) Principal Component Analysis Score Plot. (**B**) Principal Component Analysis Loading Plot. E Denotes Extreme Risk, H Denotes High Risk, and M Denotes Moderate Risk.

Table 1. Classification Scheme for Desertification Vulnerability in the Mu Us Sandy Land, Following the Criteria Proposed by Ferrara et al. (2020) [23], Showing Areal Coverage and Percentage Distribution Across Categories.

Degree of Risk	Risk Levels	Range of DSI	Area (km^2)	Percentage (%)
Low	1	1.000≤DSI≤1.170	0	0
Moderate	2	1.170 < DSI≤1.225	904.80	0.97
	3	1.225 < DSI≤1.275	710.72	0.77
High	4	1.275 < DSI≤1.325	35111.92	37.80
	5	1.325 < DSI≤1.375	35579.05	38.30
	6	1.375 < DSI≤1.425	13766.10	14.82
Extreme	7	1.425 < DSI≤1.530	5375.27	5.79
	8	1.530 < DSI≤2.000	1437.51	1.55

3.3. Analysis of the Drivers of Desertification across the Mu Us Sandy Land

Utilizing previously described sample points, our investigation into key factors affecting desertification sensitivity across the Mu Us Sandy Land implemented dual methodological approaches: K-means clustering and geographical detector technique [30,31]. These methods were used to assess the influence of the four major indicators and 13 sub-indicators on desertification sensitivity (**Figure 5**). The results indicated the hierarchical influence of principal indicators on desertification sensitivity followed this order: MQI (0.480) > VQI (0.317) > SQI (0.294) > CQI (0.165). This suggests that management quality was the most influential driver, followed by vegetation quality and soil quality, while climatic quality had the least impact.

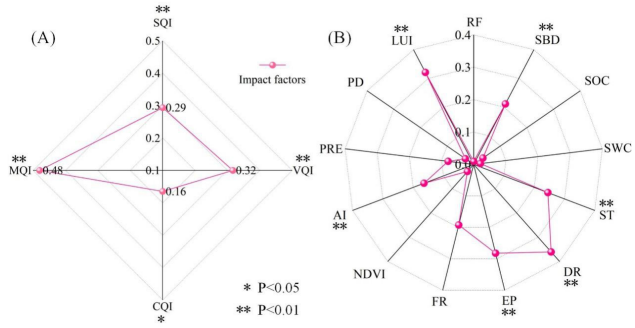

Figure 5. Assessment of Desertification Causal Mechanisms Throughout the Mu Us Sandy Land. (**A**) Driving Influence of the 4 Major Indicators on Desertification. (**B**) Driving Influence of the 13 Sub-Indicators on Desertification.

The 13 sub-indicators were ranked according to their influence on desertification sensitivity as follows: DR (0.361) > LUI (0.321) > EP (0.282) > ST (0.245) > SBD (0.211) > AI (0.164). These results indicate that DR, LUI, and EP are the primary driving factors, while ST, SBD, and AI function as secondary drivers. The remaining indicators—FR, PRE, SOC, PD, NDVI, SWC, and RF—did not exhibit statistically significant influence.

4. Discussion

4.1. Implications for Desertification Prevention Across the Mu Us Sandy Land

Our assessment of desertification vulnerability in the Mu Us Sandy Land shows strong agreement with previous studies, reinforcing the reliability of our findings. Notably, a correlation coefficient of 0.74 was observed between our results and those of Ren et al. (2024) (**Figure 6**) [28], providing indirect validation of our approach. Ji et al. (2023) similarly identified the western parts of the region—particularly Otog Banner and Otog Front Banner—as hotspots of severe desertification, aligning closely with our spatial patterns [16]. In addition, Liu et al. (2018) reported substantial land degradation across the western Mu Us Sandy Land in their spatiotemporal analysis of desertification dynamics [41]. While our study employed a different methodological framework, the consistency of these independent results supports the applicability of the MEDALUS model in this region and highlights the robustness of our desertification sensitivity assessment.

Although previous studies have indicated that desertification in the Mu Us Sandy Land has been effectively reversed due to long-term prevention and control efforts [41,42], sustained vigilance remains essential. Our findings highlight management quality as the most influential driver of desertification sensitivity, followed by vegetation and soil quality, whereas climate quality showed a comparatively limited effect. This may be attributed to the implementa-

tion of large-scale ecological restoration projects in the region—such as the conversion of farmland to forest and grassland, sand fixation through enclosure, and the planting of drought-resistant shrubs—which have significantly enhanced vegetation cover and ecosystem stability [11,12]. These interventions likely increased the system's resilience to climatic variability, thereby diminishing the direct influence of climate factors on desertification processes.

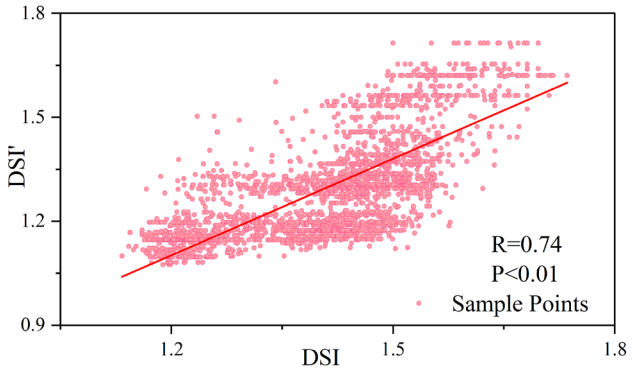

Figure 6. Comparison Between the Results of This Study and Previous Research. DSI Represents the Desertification Sensitivity Index Derived from This Study, While DSI′ Denotes the Index Values Reported in Previous Study.

Therefore, future desertification control strategies should prioritize improving management quality, alongside enhancing vegetation restoration and soil protection. First and foremost, optimizing land management is essential. In areas with poor management quality—such as the western part of Lingwu County and the northern region of Jingbian County—rational land-use planning and efficient resource allocation must be prioritized to prevent over-exploitation and unsustainable practices, particularly in grassland and farmland regions. Management strategies should incorporate crop rotation, land conservation measures, and the establishment of ecological protection zones. Furthermore, promoting sustainable land management approaches—such as ecological agriculture and grassland restoration—will help enhance ecological resilience and improve the region's overall carrying capacity. Secondly, vegetation restoration plays a pivotal role. In areas with low vegetation quality—such as the northwestern part of Otog Banner and the central-southern region of Otog Front Banner—efforts should focus on enhancing vegetation cover, particularly in zones experiencing severe degradation. Large-scale restoration projects should be implemented using native plant species well-adapted to local environmental conditions. Additionally, the establishment of windbreaks and sand fixation belts can strengthen ecosystem resilience to sandstorms and dust storms. Third, improving soil quality is critical for effective desertification control. In regions characterized by poor soil conditions—such as Wushen County, Otog Front Banner, and Yulin County—scientific soil and water conservation techniques should be applied to reduce erosion, enhance water retention and nutrient availability, and prevent soil sanding and salinization. These efforts are essential to restore soil health and reinforce its ecological functions, thereby enhancing land resilience against degradation. Although climatic factors exhibit relatively limited direct influence on desertification processes, potential consequences of atmospheric changes on hydrological systems and vegetation dynamics remain significant. Adaptive strategies to address climate-related challenges—such as improved water governance in arid regions, the development of resilient water infrastructure, and the promotion of water-efficient agricultural practices—should be prioritized to reduce the vulnerability of land systems to climate-induced degradation.

Our research results indicate that DR, LUI, and EP function as fundamental catalysts for land degradation processes across the Mu Us Sandy Land. Consequently, the desertification control strategy should focus on enhancing drought resilience, optimizing land use, and strengthening erosion control measures. Firstly, improving drought resistance is the top priority in combating desertification. In areas with low drought resistance, strategies such as planting drought-resistant species and introducing water-saving agricultural techniques should be implemented to enhance water-use efficiency. Moreover, responsible administration of subterranean aquifers alongside advocacy for water preservation behaviors remains vital for maintaining ecosystem equilibrium and perpetuity, especially during precipitation deficiency periods. Secondly, optimizing land use intensity and minimizing over-exploitation are critical to halting land degradation. Strict land-use planning and regulation should be enforced to avoid over-cultivation and overgrazing. In particular, the adoption of crop rotation, intercropping, and fallow systems should be prioritized in both farmland and grassland management, helping to maintain land productivity and enhance its resilience. Thirdly, sustainable farming practices must be encouraged

to minimize soil disturbance, and mitigate wind erosion.

4.2. Limitations and Prospects

Although our research successfully reveals the spatial pattern of desertification risk in the Mu Us Sandy Land and quantifies the drivers of desertification sensitivity, it still has some limitations. Firstly, while desertification risk is observed to increase in some agricultural and pastoral areas, this study only quantifies the impact of land use intensity without incorporating livestock pressure as a sub-indicator. Future investigations may address this gap through on-site field surveys, analysis of livestock population data, and other methods to quantitatively assess the impact of grazing intensity on land degradation susceptibility in the Mu Us Sandy Land. Secondly, the resolution of the desertification risk map generated in this study is limited to 1 km, providing only a coarse-scale, macroscopic evaluation. This resolution may obscure finer-scale spatial heterogeneity in vegetation, soil conditions, and land management practices—particularly in ecologically sensitive or fragmented landscapes. Future studies are encouraged to utilize higher-resolution remote sensing data or field-validated datasets to capture more detailed spatial patterns and enhance the precision of desertification risk assessments in this region. Thirdly, although our findings indicate that climate quality currently plays a relatively minor role in desertification sensitivity compared to management, vegetation, and soil factors, the potential long-term impacts of climate change should not be underestimated. Increasing climate variability—such as altered precipitation regimes, more frequent droughts, and rising temperatures—may influence desertification dynamics over time. Future research should incorporate temporal analyses and integrate multi-year environmental data to better evaluate the evolving influence of climate change on desertification risk in the Mu Us Sandy Land.

5. Conclusions

Employing the MEDALUS framework, our study synthesized four critical parameters—soil characteristics, vegetation attributes, climatic conditions, and management practices—to evaluate land degradation vulnerability across the Mu Us Sandy Land and investigate its causal mechanisms. Principal discoveries include:

(1) Territories exhibiting elevated degradation vulnerability encompass 71,401.70 km² (76.87%) of the Mu Us Sandy Land, demonstrating extensive geographical distribution. Zones characterized by maximum vulnerability comprise 20,578.88 km² (22.16%), predominantly situated along western boundaries of the Mu Us Sandy Land forming linear arrangements, with occasional manifestations throughout central sectors.

(2) Regarding principal assessment factors, management practices exert predominant influence on land degradation processes across the Mu Us Sandy Land, with vegetation characteristics and soil properties demonstrating secondary importance. Climate quality plays a relatively minor role in driving desertification.

(3) Among the 13 sub-indicators, drought resistance (DR), land use intensity (LUI), and erosion protection (EP) are the primary drivers of desertification sensitivity, while soil texture (ST), soil bulk density (SBD), and aridity index (AI) act as secondary drivers.

Author Contributions

Conceptualization, Y.R. and X.C.; methodology, Y.R.; validation, Y.R. and X.C.; formal analysis, Y.R. and X.C.; resources, Y.R. and X.C.; data curation, Y.R. and X.C.; writing—original draft preparation, Y.R. and X.C.; writing—review and editing, Y.R. and X.C.; visualization, Y.R. and X.C.; supervision, Y.R. and X.C.; project administration, X.C.; funding acquisition, X.C. All authors have read and agreed to the published version of the manuscript.

Funding

This work was supported by National Natural Science Foundation of China grant number [42301336] alongside Open Research Fund of Henan Provincial Key Laboratory of Hydrosphere and Watershed Water Security grant number [HWWSF202302].

Institutional Review Board Statement

Not applicable.

Informed Consent Statement

Not applicable.

Data Availability Statement

Source information references appear throughout manuscript content.

Acknowledgments

We thank the National Natural Science Foundation of China (Grant No. 42301336) and the Open Research Fund of Henan Provincial Key Laboratory of Hydrosphere and Watershed Water Security (Grant No. HWWSF202302).

Conflicts of Interest

The authors declare no conflict of interest. The funders had no role in the design of the study; in the collection, analyses, or interpretation of data; in the writing of the manuscript; or in the decision to publish the results.

Appendix A

Table A1. Classes and Corresponding Weights of Soil Sub-Indexes (Soil Bulk Density, Soil Organic Carbon, and Soil Water Content Were Classified Using the Jenks Natural Breaks Classification Method) [23,28,34,43].

Index	Class	Weight
Soil Bulk Density (g/cm^3)	<1.314	1.0
	1.314–1.437	1.1
	1.437–1.537	1.3
	1.537–1.637	1.5
	1.637–1.745	1.7
	≥1.745	2.0
Rock Fragments	≥50%	1.0
	40%–50%	1.1
	30%–40%	1.3
	20%–30%	1.5
	10%–20%	1.7
	<10%	2.0
Soil Organic Carbon	≥22.42%	1.0
	9.63%–22.42%	1.1
	3.71%–9.63%	1.3
	1.48%–3.71%	1.5
	0.37%–1.48%	1.7
	<0.37%	2.0
Soil Texture	CL; L; SCL; SL; LS	1.0
	SiCL; SiL; SC	1.2
	C; SiC; Si	1.6
	S	2.0
Soil Water Content	≥5.00%	1.0
	3.98%–5.00%	1.1
	2.99%–3.98%	1.3
	1.98%–2.99%	1.5
	0.99%–1.98%	1.7
	<0.99%	2.0

L: loam, SCL: sandy clay loam, SL: sandy loam, LS: loamy sand, CL: clay loam, SC: sandy clay, SiL: silty loam, SiCL: silty clay loam, Si: silt, C: clay, SiC: silty clay, S: sand.

Table A2. Classes and Corresponding Weights of Vegetation Sub-Indexes [23,34].

Index	Class	Weight
Drought Resistance	wooded land, shrub land, other wooded land, rivers and canals, lakes, reservoirs, permanent glacial snow, ocean	1.0
	towns, rural settlements, public transport construction land, swampy land	1.1
	open forest land, sea shoals, mudflats	1.2
	paddy field	1.4
	dry land	1.5
	grassland	1.6
	sandy land, Gobi, saline land, bare land, bare rocky gravel land, other unused land	2.0
Fire Risk	permanent glacial snow, sandy land, Gobi, saline land, bare land, bare rocky gravel land, other unused land, ocean	1.0
	other forest land, rivers and canals, lakes, reservoirs, sea shoals, mudflats, marshlands	1.1
	towns, rural settlements, public transport construction land	1.2
	forested land, shrub land, grassland	1.3
	paddy field, dry land	1.4
	open forest land	1.7
Erosion Protection	wooded land, shrub land, other wooded land, permanent glacial snow, ocean	1.0
	towns, rural settlements, public transport construction land	1.1
	rivers and canals, lakes, reservoirs, sea shoals, mudflats, marshlands	1.2
	paddy fields, open forest land	1.4
	dry land, grassland	1.7
	sandy land, Gobi, saline land, bare land, bare rocky gravel land, other unused land	2.0

Table A2. *Cont.*

Index	Class	Weight
NDVI	≥0.80	1.0
	0.72–0.80	1.1
	0.62–0.72	1.2
	0.5–0.62	1.3
	0.38–0.50	1.4
	0.26–0.38	1.5
	0.18–0.26	1.6
	0.13–0.18	1.7
	0.11–0.13	1.8
	0.10–0.11	1.9
	<0.10	2.0

Table A3. Classes and Corresponding Weights of Climate Sub-Indexes [23].

Index	Class	Weight
Precipitation (mm)	≥650	1.00
	570–650	1.05
	490–570	1.15
	440–490	1.25
	390–440	1.35
	345–390	1.50
	310–345	1.65
	280–310	1.80
	＜ 280	2.00
Aridity Index	≥1	1.00
	0.75–1	1.05
	0.65–0.75	1.15
	0.5–0.65	1.25
	0.35–0.5	1..35
	0.2–0.35	1.45
	0.1–0.2	1.55
	0.03–0.1	1.75
	＜ 0.03	2.00

Table A4. Classes and Corresponding Weights Of Management Sub-Indexes [23,34].

Index	Class	Weight
Land Use Intensity	shrubland, other woodland, permanent glacial snow, ocean	1.0
	forested land, towns, rural settlements, public transport construction land	1.1
	rivers and canals, lakes, and reservoirs	1.2
	open forest land, sea shoals, mudflat, marshland	1.3
	paddy fields	1.6
	dry land	1.7
	grassland	1.8

Table A1. *Cont.*

Index	Class	Weight
	sandy land, Gobi, saline land, bare land, bare rocky gravel land, other unused land	2.0
Population Density (inhabitants/km^2)	<4	1.0
	4–30	1.1
	30–80	1.2
	80–170	1.3
	170–300	1.4
	300–500	1.5
	500–850	1.6
	850–1400	1.7
	1400–2000	1.8
	2000–2700	1.9
	≥2700	2.0

References

[1] Sivakumar, M.V., 2007. Interactions between climate and desertification. Agricultural and Forest Meteorology. 142(2–4), 143–155. DOI: https://doi.org/10.1016/j.agrformet.2006.03.025

[2] Briassoulis, H., 2019. Combating land degradation and desertification: The land-use planning quandary. Land. 8(2), 27. DOI: https://doi.org/10.3390/land8020027

[3] Abuzaid, A.S., Abdelatif, A.D., 2022. Assessment of desertification using modified MEDALUS model in the north Nile Delta, Egypt. Geoderma. 405, 115400. DOI: https://doi.org/10.1016/j.geoderma.2021.115400

[4] Pravalie, R., Borrelli, P., Panagos, P., et al., 2024. A unifying modelling of multiple land degradation pathways in Europe. Nature Communications. 15, 3862. DOI: https://doi.org/10.1038/s41467-024-48252-x

[5] United Nations Convention to Combat Desertification, 1994. United Nations convention to combat desertification in countries experiencing serious drought and/or desertification, particularly in Africa. A/AC. 241/27, Paris, 14 October 1994.

[6] United Nations, 2012. Zero Net Land Degradation: A Sustainable Development Goal for Rio+20. UNCCD Secretariat Policy Brief. 5. United Nations Convention to Combat Desertification: Bonn, Germany; New York, USA.

[7] Bao, Y., Cheng, L., Bao, Y., et al., 2017. Desertification: China provides a solution to a global challenge. Frontiers of Agricultural Science and Engineering. 4(4), 402–413. DOI: https://doi.org/10.15302/J-FASE-2017187

[8] Yang, X., Zhang, K., Jia, B., et al., 2005. Desertifica-

tion assessment in China: An overview. Journal of Arid Environments. 63(2), 517–531. DOI: https://doi.org/10.1016/j.jaridenv.2005.03.032

[9] Zan, G., Wang, C., Li, F., et al., 2023. Key Data Results and Trend Analysis of the Sixth National Survey on Desertification and Sandification. Forest Resources Management. 1, 1–7. DOI: 10.13466/j.cnki.lyzygl.2023.01.001

[10] Lyu, Y., Shi, P., Han, G., et al., 2020. Desertification control practices in China. Sustainability. 12(8), 3258. DOI: https://doi.org/10.3390/su12083258

[11] Zhang, P., Yi, Y., Xu, J., 2021. Spatial and Temporal Characteristics of Forest and Grassland Land Use Changes After the Implementation of Grain for Green Program in China. Acta Scientiarum Naturalium Universitatis Pekinensis. 60(6), 1107–1122. DOI: https://doi.org/10.13209/j.0479-8023.2024.081

[12] Zhai, J., Wang, L., Liu, Y., et al., 2023. Assessing the effects of China's three-north shelter forest program over 40 years. Science of the Total Environment. 857, 159354. DOI: https://doi.org/10.1016/j.scitotenv.2022.159354

[13] Zhao, Y., Chi, W., Kuang, W., et al., 2020. Ecological and environmental consequences of ecological projects in the Beijing–Tianjin sand source region. Ecological Indicators. 112, 106111. DOI: https://doi.org/10.1016/j.ecolind.2020.106111

[14] Zheng, Y., Dong, L., Xia, Q., et al., 2020. Effects of revegetation on climate in the Mu Us Sandy Land of China. Science of The Total Environment. 739, 139958. DOI: https://doi.org/10.1016/j.scitotenv.2020.139958

[15] Han, X., Jia, G., Yang, G., et al., 2020. Spatiotemporal dynamic evolution and driving factors of desertification in the Mu Us Sandy Land in 30 years. Scientific Reports. 10, 21734. DOI: https://doi.org/10.1038/s41598-020-78665-9

[16] Ji, X., Yang, J., Liu, J., et al., 2023. Analysis of Spatial-Temporal Changes and Driving Forces of Desertification in the Mu Us Sandy Land from 1991 to 2021. Sustainability. 15(13), 10399. DOI: https://doi.org/10.3390/su151310399

[17] Wang, X., Song, J., Xiao, Z., et al., 2022. Desertification in the Mu Us Sandy Land in China: Response to climate change and human activity from 2000 to 2020. Geography and Sustainability. 3(2), 177–189. DOI: https://doi.org/10.1016/j.geosus.2022.06.001

[18] Li, Y., Cao, Z., Long, H., et al., 2017. Dynamic analysis of ecological environment combined with land cover and NDVI changes and implications for sustainable urban–rural development: The case of Mu Us Sandy Land, China. Journal of Cleaner Production. 142, 697–715. DOI: https://doi.org/10.1016/j.jclepro.2016.09.011

[19] Li, J., Li, Y., Wang, X., et al., 2024. Exploring the Spatial-Temporal Patterns, Drivers, and Response Strategies of Desertification in the Mu Us Desert from Multiple Regional Perspectives. Sustainability. 16(21), 9154. DOI: https://doi.org/10.3390/su16219154

[20] Lin, M., Hou, L., Qi, Z., et al., 2022. Impacts of climate change and human activities on vegetation NDVI in China's Mu Us Sandy Land during 2000–2019. Ecological Indicators. 142, 109164. DOI: https://doi.org/10.1016/j.ecolind.2022.109164

[21] Karnieli, A., Qin, Z., Wu, B., et al., 2014. Spatio-temporal dynamics of land-use and land-cover in the Mu Us sandy land, China, using the change vector analysis technique. Remote Sensing. 6(10), 9316–9339. DOI: https://doi.org/10.3390/rs6109316

[22] Dai, Z., 2010. Intensive agropastoralism: dryland degradation, the Grain-to-Green Program and islands of sustainability in the Mu Us Sandy Land of China. Agriculture, Ecosystems & Environment. 138(3–4), 249–256. DOI: https://doi.org/10.1016/j.agee.2010.05.006

[23] Wang, J., Zhang, W., Zhang, Z., 2019. Impacts of land-use changes on soil erosion in water–wind crisscross erosion region of China. Remote Sensing. 11(14), 1732. DOI: https://doi.org/10.3390/rs11141732

[24] Chen, Y., Lu, H., Wu, H., et al., 2023. Global desert variation under climatic impact during 1982–2020. Science China Earth Sciences. 66, 1062–1071. DOI: https://doi.org/10.1007/s11430-022-1052-1

[25] Kosmas, C., Kirkby, M., Geeson, N., 1999. The MEDALUS project: Mediterranean desertification and land use. Manual on key indicators of Desertification and mapping environmental sensitive areas to desertification. EUR 18882. Project ENV4 CT 95 0119. European Commission: Luxembourg.

[26] Ferrara, A., Kosmas, C., Salvati, L., et al., 2020. Updating the MEDALUS-ESA Framework for Worldwide Land Degradation and Desertification Assessment. Land Degradation & Development. 31, 1593–1607. DOI: https://doi.org/10.1002/ldr.3559

[27] Ren, Y., Zhang, B., Chen, X., et al., 2024. Analysis of spatial-temporal patterns and driving mechanisms of land desertification in China. Science of The Total Environment. 909, 168429. DOI: https://doi.org/10.1016/j.scitotenv.2023.168429

[28] Abdi, H., Williams, L.J., 2010. Principal component analysis. Wiley Interdisciplinary Reviews: Computational Statistics. 2(4), 433–459. DOI: https://doi.org/10.1002/wics.101

[29] Shafapourtehrany, M., Yariyan, P., Özener, H., et al., 2022. Evaluating the application of K-mean clustering in Earthquake vulnerability mapping of Istanbul, Turkey. International Journal of Disaster Risk Reduction. 79, 103154. DOI: https://doi.org/10.1016/

j.ijdrr.2022.103154

[30] Wang, J., Xu, C.D., 2017. Geodetector: Principle and prospective. Acta Geographica Sinica. 72, 116–134. DOI: https://doi.org/10.11821/dlxb201701010

[31] Ogbue, C., Igboeli, E., Ajaero, C., et al., 2024. Remote sensing analysis of desert sensitive areas using MEDALUS model and GIS in the Niger River Basin. Ecological Indicators. 158, 111404. DOI: https://doi.org/10.1016/j.ecolind.2023.111404

[32] Zhang, M., Wu, X., 2020. The rebound effects of recent vegetation restoration projects in Mu Us Sandy land of China. Ecological Indicators. 113, 106228. DOI: https://doi.org/10.1016/j.ecolind.2020.106228

[33] Lin, J., Bo, W., Dong, X., et al., 2024. Evolution of vegetation cover and impacts of climate change and human activities in arid regions of Northwest China: a Mu Us Sandy Land case. Environment, Development and Sustainability. 1–20. DOI: https://doi.org/10.1007/s10668-024-04704-4

[34] Ren, Y., Liu, X., Zhang, B., et al., 2023. Sensitivity Assessment of Land Desertification in China Based on Multi-Source Remote Sensing. Remote Sensing. 15(10), 2674. DOI: https://doi.org/10.3390/rs15102674

[35] Bro, R., Smilde, A.K., 2014. Principal component analysis. Analytical Methods. 6, 2812–2831. DOI: https://doi.org/10.1039/C3AY41907J

[36] Wang, X., Hua, T., Lang, L., et al., 2017. Spatial differences of aeolian desertification responses to climate in arid Asia. Global and Planetary Change. 148, 22–28. DOI: https://doi.org/10.1016/j.gloplacha.2016.11.008

[37] Wei, W., Guo, Z., Shi, P., et al., 2021. Spatiotemporal changes of land desertification sensitivity in northwest China from 2000 to 2017. Journal of Geographical Sciences. 31, 46–68. DOI: https://doi.org/10.1007/s11442-021-1832-1

[38] Bai, L., Jiang, L., Yang, D.Y., et al., 2019. Quantifying the spatial heterogeneity influences of natural and socioeconomic factors and their interactions on air pollution using the geographical detector method: a case study of the Yangtze River Economic Belt, China. Journal of Cleaner Production. 232, 692–704. DOI: https://doi.org/10.1016/j.jclepro.2019.05.342

[39] Ding, Y., Zhang, M., Qian, X., et al., 2019. Using the geographical detector technique to explore the impact of socioeconomic factors on PM2.5 concentrations in China. Journal of Cleaner Production. 211, 1480–1490. DOI: https://doi.org/10.1016/j.jclepro.2018.11.159

[40] Ikotun, A.M., Ezugwu, A.E., Abualigah, L., et al., 2023. K-means clustering algorithms: A comprehensive review, variants analysis, and advances in the era of big data. Information Sciences. 622, 178–210. DOI: https://doi.org/10.1016/j.ins.2022.11.139

[41] Liu, Q., Zhao, Y., Zhang, X., et al., 2018. Spatiotemporal patterns of desertification dynamics and desertification effects on ecosystem Services in the Mu Us Desert in China. Sustainability. 10(3), 589. DOI: https://doi.org/10.3390/su10030589

[42] Qiu, K., Xie, Y., Xu, D., et al., 2018. Ecosystem functions including soil organic carbon, total nitrogen and available potassium are crucial for vegetation recovery. Scientific Reports. 8, 7607. DOI: https://doi.org/10.1038/s41598-018-25875-x

[43] Jenks, G.F., 1967. The data model concept in statistical mapping. International Yearbook of Cartography. 7, 186–190.